APPLICATION OF TIRE DYNAMICS TO
AIRCRAFT LANDING GEAR DESIGN ANALYSIS

Raymond J. Black
Bendix Aircraft Brake and Strut Division

ABSTRACT

The tire plays a key part in many analyses used for design of aircraft landing gear. Examples include structural design of wheels, landing gear shimmy, brake whirl, chatter and squeal, complex combination of chatter and shimmy on main landing gear (MLG) systems, anti-skid performance, gear walk, and rough terrain loads and performance. This paper discusses which tire parameters are needed in the various analyses.

Two tire models are discussed for shimmy analysis, the modified Moreland approach (ref. 1) and the Von Schlippe-Dietrich approach (ref. 2). It is shown that the Moreland model can be derived from the Von Schlippe-Dietrich model by certain approximations.

The remaining analysis areas are discussed in general terms and the tire parameters needed for each are identified. The conclusion of the paper is that accurate tire data allows more accurate design analysis and the correct prediction of dynamic performance of aircraft landing gear.

INTRODUCTION

A number of important design analysis areas of aircraft landing gear require accurate data on tire dynamic parameters. One of the more obvious examples is wheel design. The primary loads acting on the wheel act through the tire onto the wheel bead seat area. The wheel cannot be efficiently designed without accurate data on tire to wheel contact loads for the entire spectrum of operating conditions to which the landing gear system is subjected. This includes landing impact, braked roll, taxiing, turning, cross wind landing, and in some cases obstacle impact. The latter is particularly true for carrier based airplanes. The wheels of such aircraft must accommodate running over arresting cables when the tire is in the near bottomed condition. Modern aircraft wheel design makes use of experimentally and analytically determined bead contact forces to arrive at optimized designs of the wheel cross sections. In spite of increased demands for more durable wheels having longer fatigue life and increased capabilities, wheel weight per unit load has decreased in recent years.

Other design analysis areas involving the entire landing gear system include:

- Landing gear shimmy (both nose and main landing gear)
- Brake-landing gear whirl stability
- Brake chatter and squeal
- Complex combinations of chatter and shimmy
- Anti-skid performance
- Gear walk
- Rough terrain operations

This paper will concentrate primarily on the tire parameters needed in the first four of the above problem areas.

LANDING GEAR SHIMMY

There are two tire models commonly used for aircraft landing gear shimmy analysis: the modified Moreland model (refs. 1, 3, and 4) and the Von Schlippe-Dietrich model (refs. 2, 5, and 6). The equations for the forces and moments at the tire footprint are similar for the currently used versions of the two models and as a result there are a large number of parameters which are common to both models. Both models require that the vertical load deflection characteristics of the tire be known along with the general load, inflation pressure and speed envelope of operation of the aircraft. In addition the following parameters must be known for the operational envelope:

m_t = mass of tire (kg)

I_{pt} = polar moment of inertia of inflated tire (kg·m^2)

I_{dt} = diametral moment of inertia of inflated tire (kg·m^2)

K_1 = lateral spring rate of tire (N/m)

C_L = lateral equivalent viscous damping coefficient (N·sec/m)

μ_1 = rolling tire torsional spring rate (N-m/m)

μ_D = rolling tire torsional damping coefficient (N·m/sec)

R_g = loaded radius of the tire (m)

C_w = slope of drag force versus slip ratio for small slip ratios (N)

R_r = tire rolling radius (m)

For the modified Moreland model, two additional parameters are required:

C = coefficient of yaw (rad/N)

C_1 = yaw time constant (sec)

These parameters are used in Moreland's cornering relationship:

$$CF_{nj} = \psi_{tj} + c_1 \dot{\psi}_{tj} \tag{1}$$

where

    j = index indicating the jth wheel of a multi-wheel landing gear

    F_{nj} = lateral force acting on tire footprint (N)

    ψ_{tj} = yaw angle or sideslip angle of tire footprint with respect to the tire (rad)

Dots over a variable are used to indicate differentiation with respect to time.

In the Von Schlippe-Dietrich model it is shown that the cornering characteristics come about due to continuity between the tire distortion in the footprint's most forward position and the lateral distortion of the tire as a function of peripheral distance, combined with adhesion of the tire footprint centerline to the ground surface. Denoting the lateral displacement of the tire outside the footprint as λ and the peripheral distance around the tire as s (s = 0 corresponds to the forward tip of the footprint and s > 0 corresponds to moving upward around the tire center) it is found from experiments that when a pure lateral load is applied to the tire λ is given by

$$\lambda = \lambda_p \left(a_1 e^{-s/L} + (1-a_1) \right) \qquad (2)$$

where λ_p = lateral deflection of footprint (constant within footprint) (m)

    s = peripheral distance (m)

    a_1 = experimental constant between zero and 1 (dimensionless)

    L = experimentally determined "relaxation" length (m)

    For type VII tires, a_1 is very close to 1. However, for many new design tires with a relatively small aspect ratio and a relatively small width between wheel flanges, a_1 is significantly less than unity. For example, on a H45 x 17-20, PR22 tire, typical values of a_1 range from 0.80 to 0.92, depending on the vertical load and the tire pressure.

As a consequence of Equation (2), it can be shown that when the wheel moves forward an amount ds the most forward position of the tire footprint will move an amount

$$d\lambda_1 = \lambda_p \frac{a_1}{L} ds \qquad (3)$$

relative to its position prior to rolling forward. The quantity a_1/L is denoted by

$$c_\lambda = a_1/L \tag{4}$$

It can be shown that as a consequence of Equation (2) the steady state "cornering power" or cornering coefficient is given by

$$N = \frac{1}{2} \frac{K_1}{C_\lambda} \left(1 + e^{2C_\lambda h}\right) \tag{5}$$

where

N = cornering coefficient (N/rad)

C_λ = tire coefficient defined by Equation (4), (1/m)

h = half length of the tire footprint (m)

For transient conditions the general kinematic situation is illustrated in Figure 1. Due to strut deflection, the wheel is tilted at an angle ϕ_B and twisted in the yaw direction at an angle ψ_s' . The coordinate of the wheel axle center is y_a and the coordinate of the most forward position of the tire footprint is y_{fp}. The wheel is rolled forward an amount ds during which time the position variables of the tire change by amounts $d\phi_B'$, $d\psi_s'$, dy_a, $d\lambda$, and $C_\lambda \lambda$ ds as defined by Equations (3) and (4).
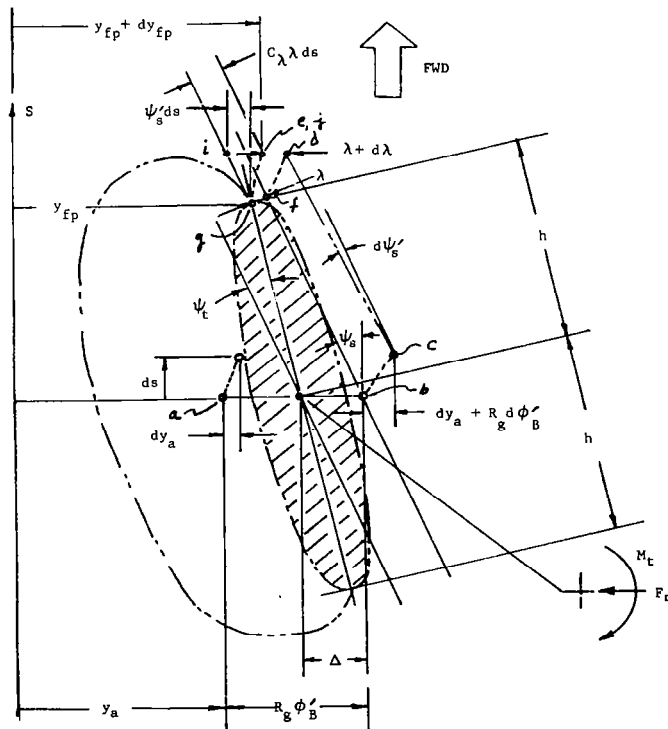

Figure 1.- Tire distortion nomenclature.

With this in mind we can, from Figure 1, write the quantity $y_{fp} + dy_{fp}$ in two ways. We first consider the path a to b to c to d to e which gives

$$y_{fp} + dy_{fp} = y_a + R_g \phi_B' + dy_a + R_g d\phi_B' - h(\psi_s' + d\psi_s') - (\lambda + d\lambda) \quad (6)$$

Next, we consider the path a to b to f to g to i to j which gives

$$y_{fp} + dy_{fp} = y_a + R_g \phi_B' - h\psi_s' - \lambda - \psi_s' ds + c_\lambda \lambda ds \quad (7)$$

Equating (6) to (7) gives

$$dy_a + R_g d\phi_B' - hd\psi_s' - d\lambda = - \psi_s' ds + c_\lambda \lambda ds \quad (8)$$

which can be written as

$$\frac{d\lambda}{ds} + c_\lambda \lambda = \frac{dy_a}{ds} + R_g \frac{d\phi_B'}{ds} + \psi_s' - h \frac{d\psi_s'}{ds} \quad (9)$$

We can eliminate λ from Equation (9) by defining λ in terms of y_a and y_{fp}. Again from Figure 1,

$$\lambda = y_a - y_{fp} + R_g \phi_B' - h\psi_s' \quad (10)$$

Substituting (10) into (9) gives

$$\frac{dy_{fp}}{ds} + c_\lambda y_{fp} = c_\lambda (y_a + R_g \phi_B') - (1 + c_\lambda h) \psi_s' \quad (11)$$

Or, letting $\frac{d}{ds} = D$, this substitution will yield

$$y_{fp} = \frac{1}{D + c_\lambda} \left[c_\lambda \left(y_a + R_g \phi_B' \right) - \left(1 + c_\lambda h \right) \psi_s' \right] \quad (12)$$

As a result of adhesion of the tire footprint to the ground, we can write

$$y_{fp}(s = -h) = y_a + R_g \phi_B' - \Delta \quad (13)$$

76

Taking the series expansion for the left hand side of Equation (13) gives

$$y_{fp}(s = -h) = y_{fp} - h \frac{dy_{fp}}{ds} + \frac{h^2}{2!} \frac{d^2 y_{fp}}{ds^2} - \cdots \tag{14}$$

Applying (14) to (12) and making the substitution $D = \frac{1}{v} D_t$ where $D_t = d/dt$ gives

$$\left(1 - \frac{h}{v} D_t + \frac{h^2}{2!v^2} D_t^2 - \frac{h^3}{3!v^3} D_t^3 + \cdots\right)\left(c_\lambda (y_a + R_g \phi_B') - (1 + c_\lambda h) \psi_s'\right) =$$
$$\left(\frac{D_t}{v} + c_\lambda\right)\left(y_a + R_g \phi_B' - \Delta\right) \tag{15}$$

Equation (15) is the basic cornering relationship used in the current version of the Von-Schlippe-Dietrich tire model.

Although Equation (15) does not appear to resemble the Moreland cornering relationship, it can be shown that they are similar. If the infinite series representing the distance delay is restricted to the first two terms, $1 - (h/v)D_t$, and the following kinematic relationship is introduced:

$$V(\psi_s - \psi_t) = -D_t(y_a + R_g \phi_B' - \Delta) \tag{16}$$

where V is the forward velocity of the airplane, then Equation (15) can be rewritten as:

$$\Delta = \left(\frac{1 + hC_\lambda}{C_\lambda}\right) \dot{\psi}_t + \frac{h}{v}\left(\dot{\Delta} - \frac{(1 + hC_\lambda)}{C_\lambda} \dot{\psi}_s'\right) \tag{17}$$

Since the side force is given by

$$F_n = K_1 \Delta + C_L \dot{\Delta} \tag{18}$$

Equation (17) can be written

$$\frac{C_\lambda}{K_1(1 + hC_\lambda)} F_n = \dot{\psi}_t + \frac{C_L}{K_1} \dot{\psi}_t + \frac{C_\lambda h(K_1 + C_L D_t)}{VK_1(1 + hC_\lambda)}\left(\dot{\Delta} - \frac{(1 + C_\lambda h)}{C_\lambda} \dot{\psi}_s'\right) \tag{19}$$

For large values of V the far right hand term is small. Thus Equation (19) is similar to Equation (1) with

$$\frac{C_\lambda}{K_1\left(1 + hC_\lambda\right)} \approx C \quad \text{or} \quad \frac{1}{N} \quad \text{from Equation (5)} \tag{20}$$

$$\text{and} \quad \frac{C_L}{K_1} \approx C_1 \tag{21}$$

From the latter it is apparent that Moreland's cornering relationship is equivalent to an approximation of the Von Schlippe-Dietrich model. This explains why the two models give similar results when used in shimmy analysis. It has been found that in many cases the Moreland model is slightly more unstable than the Von Schlippe-Dietrich model. It is often more conservative to use the Moreland model for landing gear design. Moreland's model is also more simple from a computational standpoint since one does not have to deal with the infinite series or, equivalently, the time delay function represented by Equations (14) and (13) respectively.

The forces acting at the tire footprint are only part of the shimmy problem formulation. Figure 2 illustrates the factors considered in the total problem, namely the airplane, the local structure between the airplane and the landing gear, the landing gear structure, and finally the footprint of the tire.

The fuselage is represented by the three dimensional motion of a fuselage reference point. The three motions are a lateral motion y_f, a roll motion ϕ_f, and a yaw motion ψ_f. Three input forces corresponding to these three directions act from the landing gear. The motion of the fuselage is given by solution to model equations covering the first several normal modes of the fuselage. The equation of motion of the fuselage is:

$$[M] \begin{Bmatrix} \ddot{q} \end{Bmatrix} + (1 + i\eta_f) [K] \begin{Bmatrix} q \end{Bmatrix} = [\delta] \begin{Bmatrix} Fy_a \\ T_{\psi a} \\ T_{\phi a} \end{Bmatrix} \qquad (22)$$
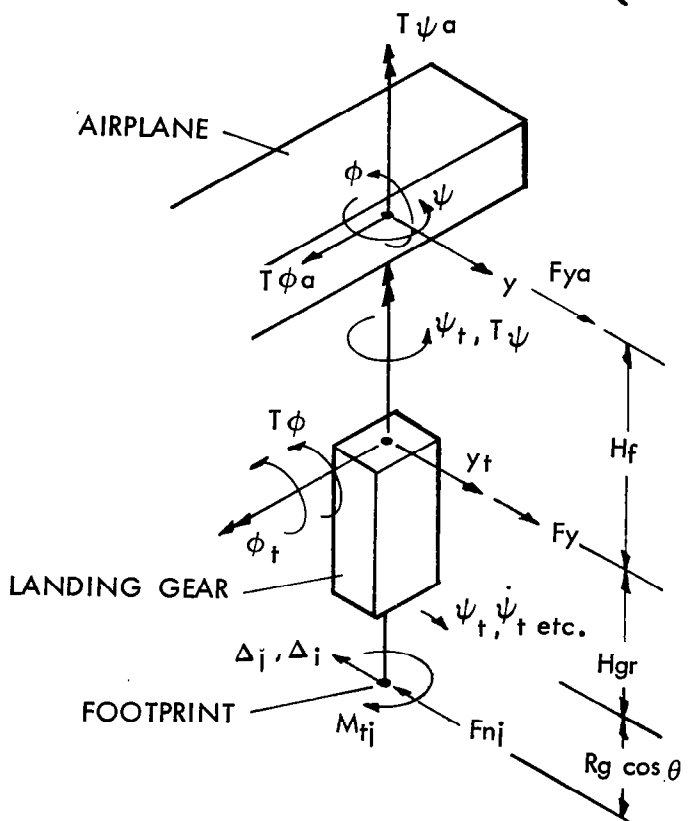

Figure 2.- Shimmy modeling considerations.

where

$[M]$ = fuselage modal mass matrix (kg)

$[K]$ = fuselage stiffness matrix (N/m)

n_f = loss factor for fuselage structure

$[\delta]$ = modal deflection matrix

$\left.\begin{array}{c} F_{ya} \\ T_{\psi a} \\ T_{\phi a} \end{array}\right\}$ forces and moments in the y, ψ and ϕ directions

q = vector of n normal modes

To obtain the fuselage deflection at the reference point the q vector is multiplied by the transpose of the modal deflection matrix.

$$\left\{\begin{array}{c} y_f \\ \psi_f \\ \phi_f \end{array}\right\} = [\delta]^T \left\{\begin{array}{c} q_1 \\ q_2 \\ \vdots \\ q_n \end{array}\right\} \tag{23}$$

The relative deflections due to the structure from the fuselage reference point to the landing gear attach point are given by:

$$\left\{\begin{array}{c} y_t - y_f \\ \psi_t - \psi_f \\ \phi_t - \phi_f \end{array}\right\} = [f] \left\{\begin{array}{c} F_y \\ T_\psi \\ T_\phi \end{array}\right\} \tag{24}$$

where

$$\left\{ \begin{array}{c} y_t - y_f \\ \psi_t - \psi_f \\ \phi_t - \phi_f \end{array} \right\} = \text{relative deflections in the } y, \psi \text{ and } \phi \text{ directions}$$

$$[f] = \text{flexibility matrix}$$

$$\left\{ \begin{array}{c} F_y \\ T_\psi \\ T_\phi \end{array} \right\} = \text{forces and moments in the } y, \psi, \text{ and } \phi \text{ directions}$$

The mathematical model of the landing gear is fairly straightforward. Care must be taken in properly accounting for cross coupling of flexibilities and inertial cross coupling brought on by off-center masses of the landing gear system such as torque arms, steering cylinders, lights and attachment fittings. Since each gear differs in details the equations of motion will not be given here.

The remaining equations are those of the tire forces and kinematic restraints. For both the Moreland and Von Schlippe-Dietrich models, these equations are:

$$F_{nj} = K_1 \Delta_j + C_L \dot{\Delta}_j \tag{25}$$

for the side force,

$$M_j = \mu_1 \psi_{tj} + \mu_{1D} \dot{\psi}_{tj} \tag{26}$$

for the moment, and

$$V(\psi_s' - \psi_{tj}) = -\dot{y}_a - R_g \dot{\phi}_B' + \dot{\Delta}_j \tag{27}$$

for the kinematic constraint.

80

For the Moreland tire model the tire equations are completed using Equation (1) as the final relationship while for the Von Schlippe-Dietrich model Equation (15) is used.

For dual wheel landing gear systems there is an additional moment acting from the ground about an axis normal to the ground plane. This moment, M_w, is governed by the following differential equation:

$$\dot{M}_w + (C_w R_r R_g / V I_p)\, M_w + 2K_w/I_p \int M_w\, dt = -(C_w l_s^2/2V)\, \ddot{\psi}_s' - K_w C_w l_s^2/V I_p\, \psi_s' \qquad (28)$$

where in addition to previously defined parameters

$\quad I_p$ = polar moment of inertia of one wheel and tire $(kg \cdot m^2)$

$\quad l_s$ = distance between wheel centerlines (m)

$\quad K_w$ = torsional spring rate of corotational axle $(N \cdot m)$

If K_w = 0 then Equation (28) still may be used by simply setting K_w = 0 and retaining the remaining terms. It can be noted that an additional tire parameter, C_w, is needed to deal with dual wheel landing gear systems. This parameter defines the tire drag forces in terms of the percent tire slip for small slip ratios.

Figure 3 shows the Space Shuttle nose landing gear (NLG), which was analyzed extensively for shimmy stability using computerized solutions of the equations of motion previously described, dynamometer testing, and "runway" tests on the Langley Landing Loads Track. This work was extremely important since there were no high-speed taxi tests in the Space Shuttle development program. The first "test" of the landing gear was an actual landing at over 200 mph.

The computer study was used to select the optimum damping for the steer damp unit, to determine sensitivity to wear, friction, and tire parameters, and generally to establish what the margin of stability was for the landing gear system. This was then verified and improved upon by the dynamometer test. Application to a flat runway was verified by comparison of dynamometer and Langley Landing Loads Track test results. The Langley Landing Loads Track could not be used for the full range of speeds and vertical loads because of limitations on track capacity. The dynamometer tests covered the full range of speeds and loads.

Figure 4 demonstrates, for a typical case, the correlation between the computer analysis and the dynamometer (120" flywheel) results. Figure 5 shows the correlation between the dynamometer tests and the NASA dry concrete runway data from the Langley Landing Loads Track. Both sets of results correlate closely, showing that the analytical model can be used with confidence for prediction of the Space Shuttle NLG's stability over a wide range of landing and roll-out conditions.

The process of test and analysis for shimmy stability is described in Reference 7.
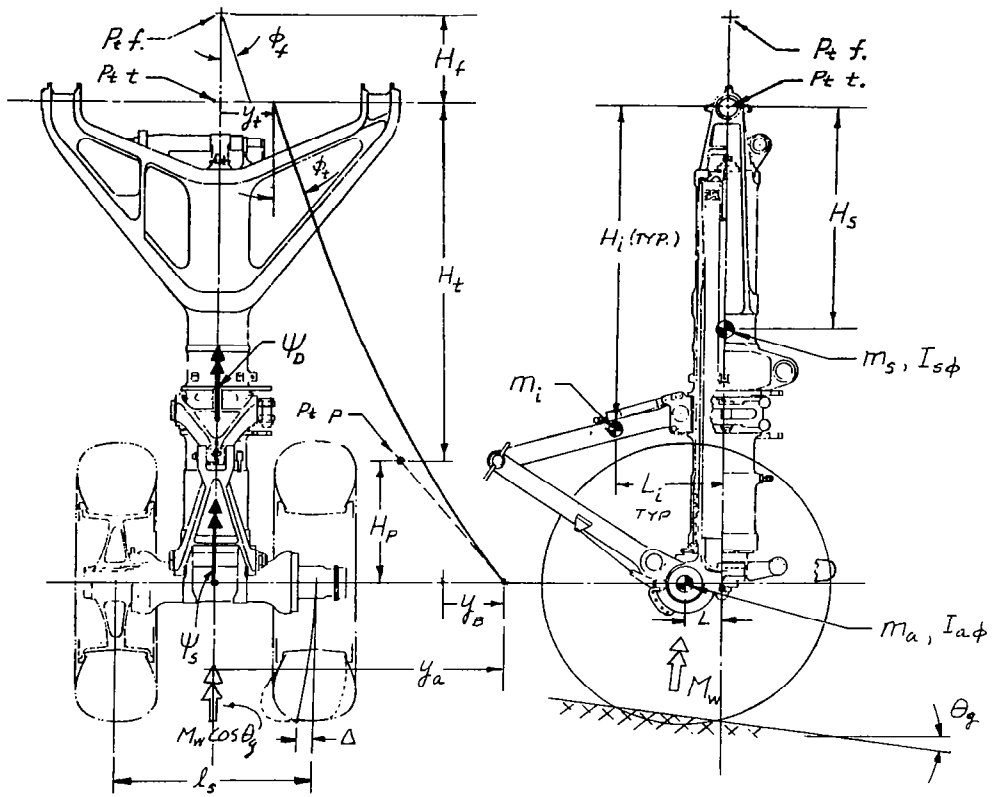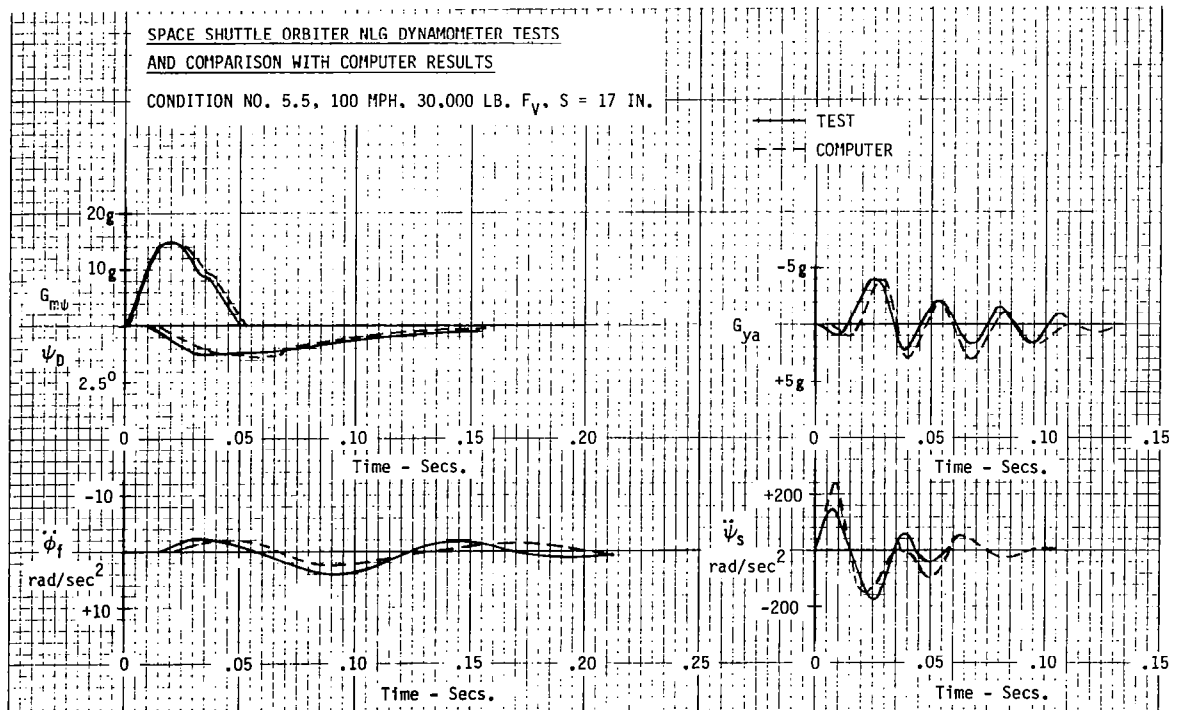
Figure 3.- Space Shuttle NLG.

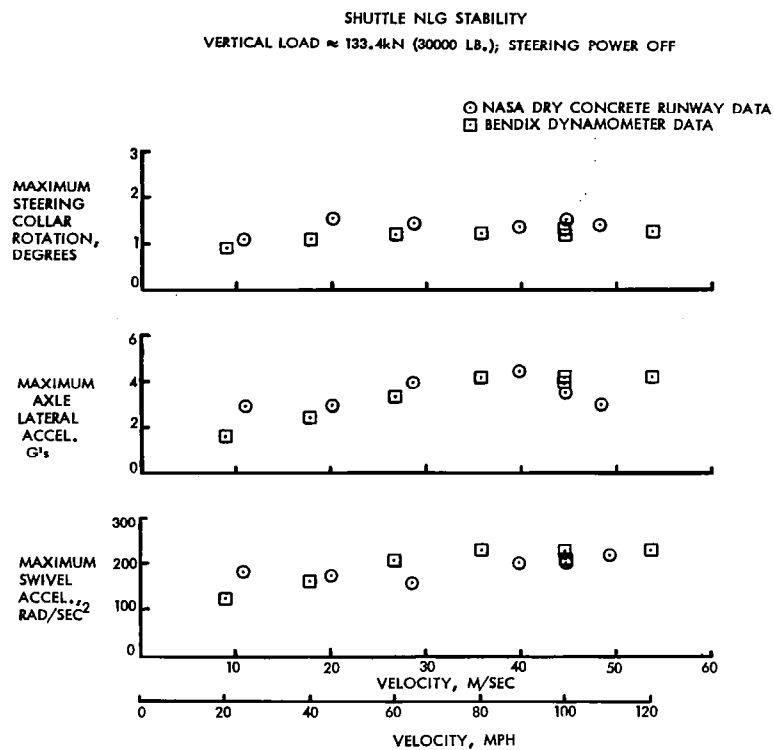Figure 4.- Correlation between dynamometer and analytical results.

SHUTTLE NLG STABILITY

VERTICAL LOAD ≈ 133.4kN (30000 LB.); STEERING POWER OFF

⊙ NASA DRY CONCRETE RUNWAY DATA
◻ BENDIX DYNAMOMETER DATA

Figure 5.- Correlation between dynamometer and dry concrete
runway data.

MAIN LANDING GEAR SHIMMY

In addition to NLG's, shimmy can be encountered on main landing gear systems (MLG's). Three very popular commercial jet aircraft having dual wheel main landing gears experienced similar MLG shimmy problems when they were first introduced. The problem was traced to a side brace configuration which caused twist in the landing gear due to application of a side load. The side braces were all connected to the forward part of the shock strut for the three different aircraft. Modifications were made to the MLG's to stabilize the systems. In two cases a torque arm damper was introduced while in the third case a negative (forward) mechanical trail was used to stabilize the shimmy.

In general MLG's are more complex than NLG's; however, the same tire parameters are needed for MLG stability studies as are used for NLG's. The complexity is associated with the landing gear structure itself. This is illustrated in Figure 6 which is a drawing of the six wheeled C5A MLG. The analysis of this system used a 48 degree of freedom analysis reduced to a twelve degree of freedom system for non-linear simulation studies. The 48 degrees of freedom were necessary to develop an accurate mass and stiffness matrix for the reduced system.

Sample stability results are given in Figure 7 and illustrate the importance of accurate tire parameters. Here the only difference between the two runs is the yaw time constant. The solid curve corresponds to a yaw time constant (C_1) of 0.06 seconds while the dotted curve applies to a C_1 value of 0.03 seconds. The actual yaw time constant for the 49 x 17 tires is considerably lower than both of these values but the comparison served to show the sensitivity of shimmy stability to tire parameters.
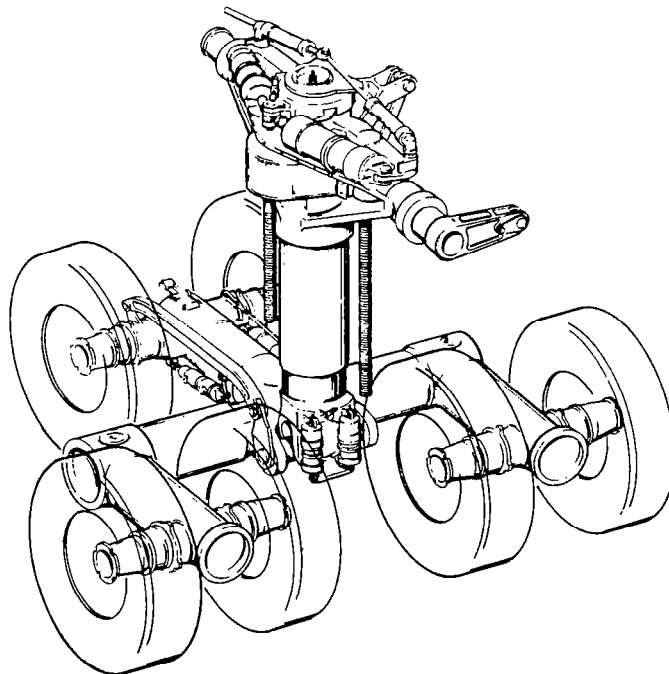

Figure 6.- C5A main landing gear.

The net result of the shimmy stability study showed the C5A MLG to be stable, a result which was later verified by in-service experience. The analysis was important since this was the first time that this six wheeled landing gear configuration was used on an aircraft.

The diversity of MLG designs is illustrated by the complex single wheel MLG shown in Figure 8. This was a preliminary design for the gear which was complicated by the fact that it had to retract around a wing mounted rocket. Needless to say no single set of equations of motion suffice to cover all landing gear systems. Fortunately, however, the tire parameters previously given apply to all landing gears.
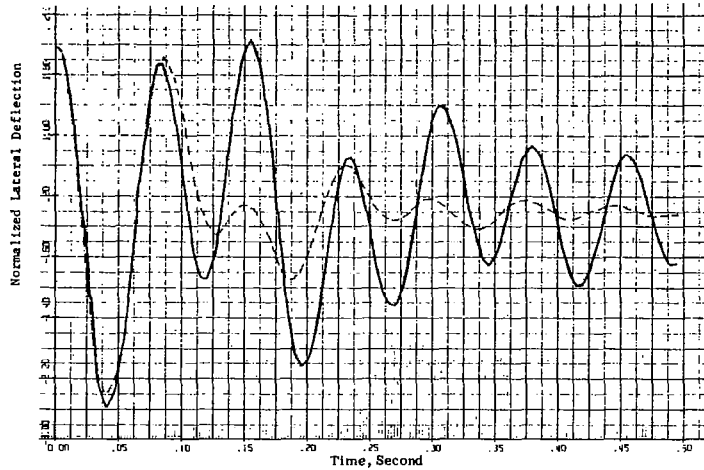
Figure 7.- Comparison of transient motion for two values
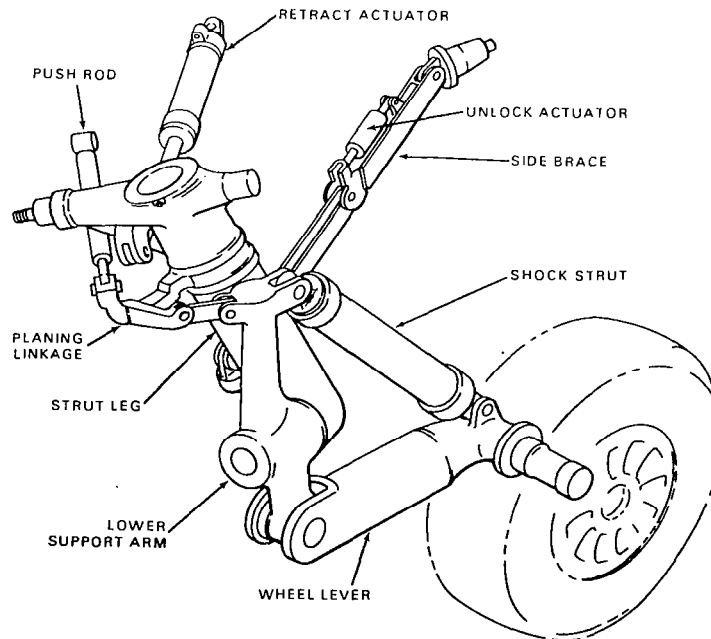of the yaw time constant (C5A MLG).

Figure 8.- Single wheel MLG design for a fighter aircraft.

BRAKE WHIRL

Brake whirl is a highly destructive self excited vibration of the wheel, tire, brake and landing gear structure. It is caused by a localized high pressure region in the brake stack that brings about out of plane bending of the axle. The resulting motion is characterized by a sinusoidal bending of the axle which takes place in two planes, the z-y plane and the x-y plane, as shown in Figure 9. The two motions are 90° out of phase which makes it appear that the bending motion is whirling about the axle centerline at a speed corresponding to the radial natural frequency.

The mathematical analysis of the brake whirl problem requires that a number of tire properties be known. Since the frequency of the whirl motion is generally in the range of 200 to 400 Hz for most landing gears the tire does not respond as it does for low frequency motions. The tire tread remains fixed in the x-z plane except for its steady forward motion and rotation. The heavy bead area of the tire moves with the wheel adding to its effective mass and its moments of inertia. The region between the tread and the wheel is treated as a spring with radial and angular spring constants and associated loss factors.
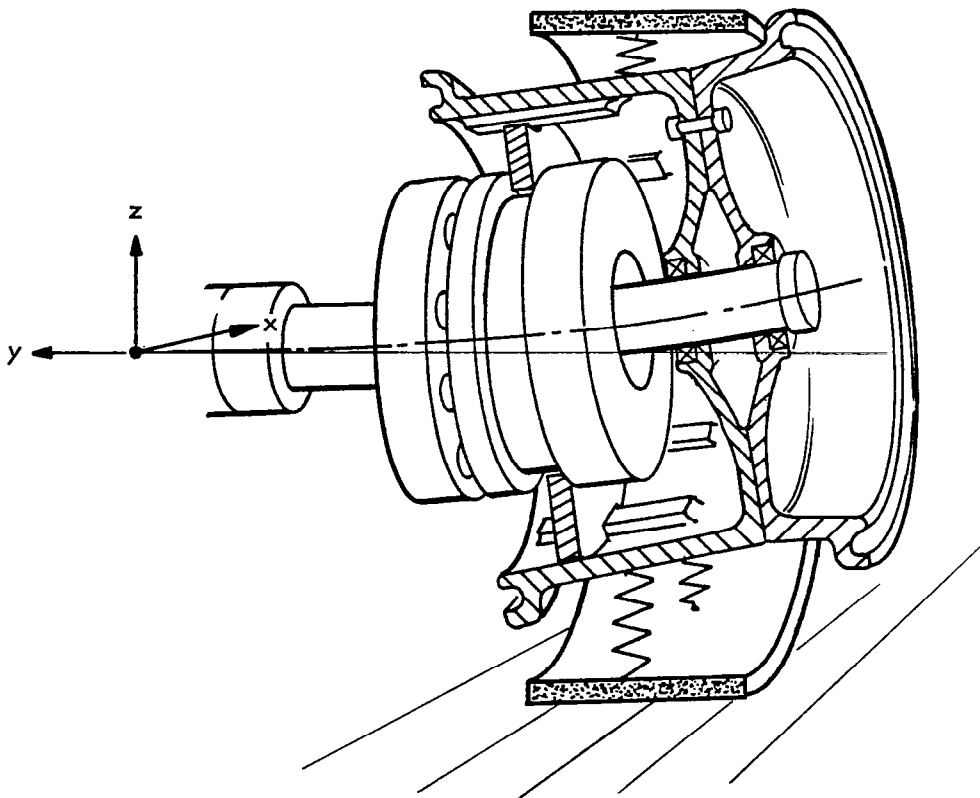

Figure 9.- Brake whirl.

The specific tire parameters are:

K_r = spring rate of tire associated with radial displacement of the wheel with the tread held fixed (N/m)

η_r = loss factor associated with K_r

K_α = diametral angular spring rate of the tire associated with twist of the wheel with the tread held fixed (N·m/rad)

$\eta_{\alpha r}$ = loss factor associated with K_α

M_{tw} = mass of the tire moving with the wheel (the bead area of the tire) (kg)

I_p = polar moment of inertia of m_{tw} (kg·m^2)

I_{dt} = diametral moment of inertia of M_{tw} (kg·m^2)

R_r = tire rolling radius (m)

Brake whirl stability is a somewhat more serious problem on carbon brake systems because of their mass distribution properties. A careful analysis as well as design changes to stabilize the motion are important in the initial stages of the brake development.

Measurement of the tire stiffness parameters is difficult. As a first approximation K_r is taken to be the average of the fore and aft tire stiffness and the vertical stiffness of the tire. The value of K_α is calculated based on lateral deformation of the tire at both the footprint and 180° from the footprint. The loss factor is estimated to be approximately 0.15 for typical aircraft tires. The mass M_{tw} is roughly 30% of the tire for typical aircraft tires. Calculation of I_p and I_{dt} can be carried out knowing M_{tw} and the location of the bead bundle. The rolling radius can be determined by conventional methods and is equal to the undeflected radius of the tire minus one-third of the tire deflection as a very close approximation.

BRAKE CHATTER AND SQUEAL

Brake chatter and squeal are self excited motions of the brake and landing gear system brought on by so called negative damping at the rotor-stator interface. The negative damping results from an increase in brake torque for a decrease in the instantaneous brake slip velocity. This characteristic yields a term in the equations of motion which looks like a damping term in that it is a force or torque proportional to velocity, but has a sign opposite to that of the dissipative damping of the motion. Thus, the lining characteristic has been termed negative damping.

The chatter motion is a low frequency motion (5 Hz to 15 Hz) and consists of fore and aft bending motion of the shock strut. Squeal consists of wind-up of the stationary parts against the torque take-out system and has a natural frequency of 150 to 500 Hz.

A relatively simple model of brake chatter and squeal uses three degrees of freedom. These are the fore and aft bending motion of the landing gear shock strut, the torsional wind-up of the nonrotating parts of the brake against the torque take-out system, and the forward velocity of the airplane. The nonrotating parts of the brake consist of the brake piston housing, the pressure plate, the backing plate, the stators of the brake, and the torque tube of the brake which carries the stators. The torque take-out system consist of an axle flange on most single and dual wheel landing gears and a brake equalizer rod on truck type landing gears commonly used on larger aircraft.

The tire parameters used in the simplified chatter and squeal analysis consist of the following:

R_r = tire rolling radius (m)

R_g = loaded radius of tire (m)

C_w = slope of drag force versus slip ratio for small slip ratios (N)

M_t = mass of tire (kg)

I_p = polar moment of inertia of tire (kg·m^2)

C_x = ratio between the shift in the center of pressure and the aft deflection of the footprint

This three degree of freedom analysis is quite simplified but is useful for preliminary studies of stability of chatter and squeal, particularly for the selection of lining materials that will not result in self-excitation of the vibratory motions. At a later stage in the landing gear development, a more detailed analysis of brake chatter and squeal such as the one that is described in the next section can be carried out.

COMPLEX COMBINATIONS OF CHATTER AND SHIMMY

For most modern main landing gear systems the chatter motion is not simply a fore and aft bending action of the shock strut but rather consists of a complex motion of the gear involving fore and aft, lateral, roll, and yaw motions of the gear. Thus many of the same tire parameters that are used in shimmy analysis are also needed for an analysis of the brake chatter and squeal.

Figure 10 shows a typical truck type main landing gear system and some of the nomenclature and motions considered. There are ten degrees of freedom in the model:

x_B = aft deflection at the truck pivot point (m)

y_B = lateral deflection at the truck pivot point (m)

ϕ_B = roll angle of truck (rad)

θ_B = end bending angle of shock strut (rad)

ψ_B = yaw angle of truck (rad)

ω_1 = angular velocity of one of the forward wheels (rad/sec)

ω_3 = angular velocity of one of the aft wheels (rad/sec)

θ_{s1} = angular rotation of the forward brake stationary parts (rad)

θ_{s3} = angular rotation of the aft brake stationary parts (rad)

x_p = forward translational motion of airplane (m)

A fairly extensive set of tire parameters is needed for the model. The shimmy action uses the simple cornering relationship equating the tire lateral force to a sideslip angle divided by the coefficient of yaw. This is equivalent to the modified Moreland model with $C_1 = 0$.

The tire parameters used in the model are:

K_x = fore and aft tire spring rate (N/m)

K_z = vertical tire spring rate (N/m)

C = coefficient of yaw (rad/N)

μ_ψ = lateral coefficient of friction between tire and runway, a function of slip ratio

$\mu_{\psi m}$ = maximum value of μ_ψ

μ_1 = ratio between self-aligning torque and sideslip angle (N·m/rad)

μ_x = maximum fore and aft coefficient of friction between tire and runway

C_w = ratio between the drag force and the slip ratio for small slip ratios (N)

C_x = ratio between the shift in the center of pressure and the aft deflection of the tire

M_t = mass of tire (kg)

I_{pt} = polar moment of inertia of inflated tire (kg·m^2)

I_{dt} = diametral moment of inertia (kg·m^2)

R_g = loaded radius of tire (m)

R_r = rolling radius of tire (m)

A sample result of the nonlinear analysis is shown in Figure 11. In this run the negative damping from the brake lining was set relatively high and the system damping, made up of several nonlinear terms, was set at about one half the expected value. A pulse was added to the torque to cause excitation at the midpoint of the 10 mph stop. It can be seen in Figure 11 that the initial motion is stable but that the pulse causes enough disturbance that the resulting motion is near neutral stability. The mode shape of the motion is far from a simple fore and aft truck motion. Note that the lateral motion of the truck is the same order of magnitude as the aft motion of the truck. Also, there is some yaw motion and considerable roll motion of the truck.

Studies of this type help to establish the amount of negative damping that can be tolerated by both the chatter motion and the high frequency squeal motion of the landing gear. Also mode shapes and frequencies of the several low frequency chatter motions can be established together with the margin of stability of each mode.
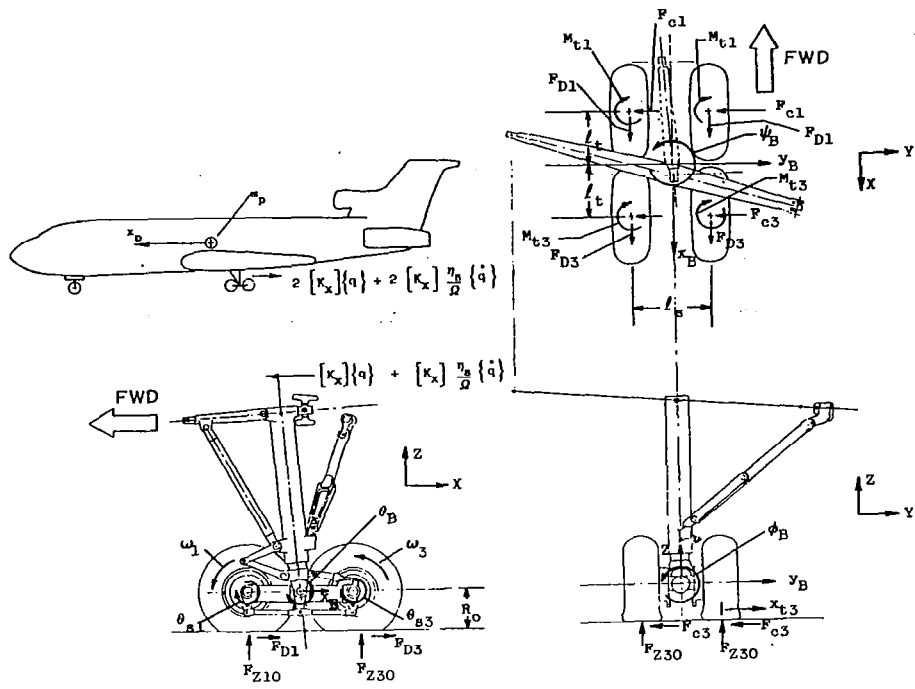
$$2 \left[\kappa_x \right]\{q\} + 2 \left[\kappa_x \right] \frac{\eta_B}{\Omega} \{\dot{q}\}$$

$$\left[\kappa_x \right]\{q\} + \left[\kappa_x \right] \frac{\eta_B}{\Omega} \{\dot{q}\}$$

FWD

Figure 10.- Nomenclature and motions for complex chatter and shimmy analytical model.

BENDIX ENCO   RUN NO. 020

7.5% OF CRIT. DAMP.

x_B = AFT MOTION OF TRUCK

ψ_B = SWIVEL (YAW) MOTION OF TRUCK

y_B = LATERAL MOTION OF TRUCK

ϕ_B = ROLL MOTION OF TRUCK

θ_B = END ANGLE ON SHOCK STRUT (PITCH)

SECONDS

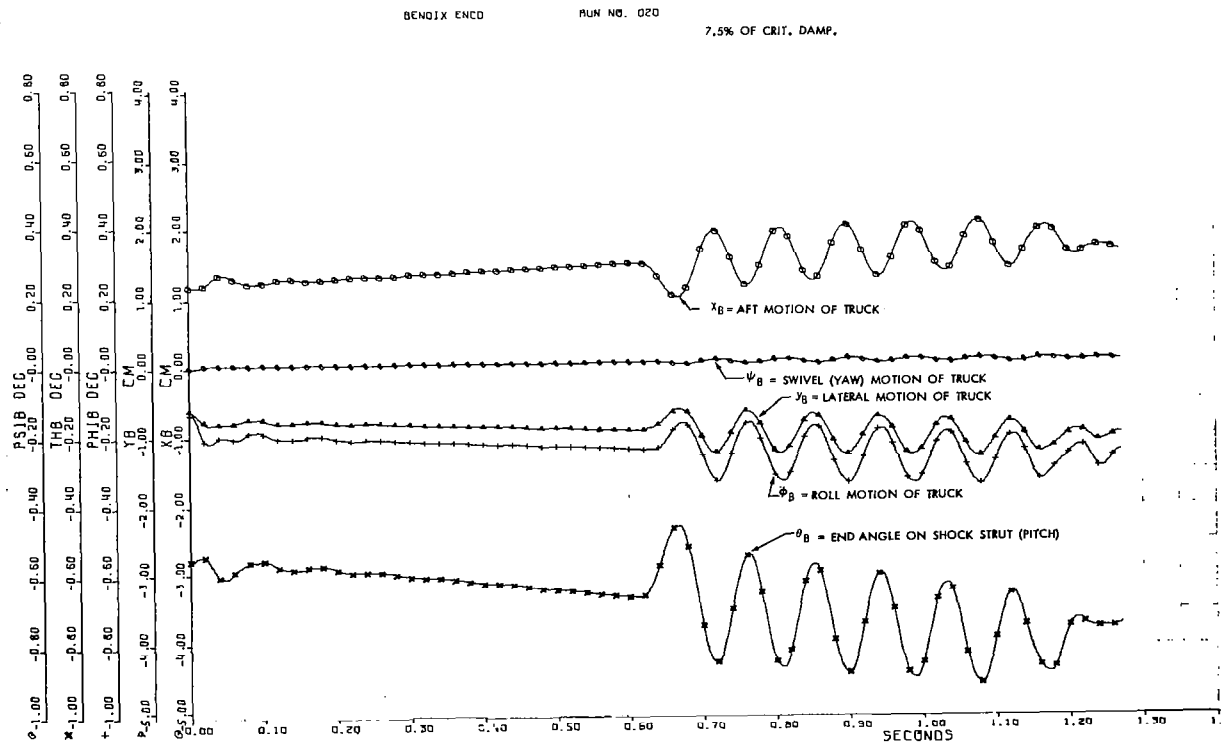PSIB DEG   THB DEG   PHIB DEG   YB CM   XB CM

Figure 11.- Sample computer run for MLG chatter and shimmy analytical model.

OTHER ANALYSIS AREAS

The other analysis areas mentioned at the beginning of this paper also require detailed information on tire characteristics. Anti-skid performance requires a model of the brake pressure to brake torque transfer function along with the dynamic characteristics of the anti-skid system. The remainder of the model is similar to that used for chatter and squeal. Gear walk which is a stick-slip motion similar to chatter can come about due to stick-slip action at either the ground surface or the brake interfaces. Rough terrain operations require a tire model capable of predicting vertical and drag loads due to obstacle or hole impact at obstacle lengths which range from a small fraction of the footprint length up to several times the footprint length. The short lengths present more of a problem but methods are available for predictions of tire loads for all lengths. Rough terrain operations analysis also requires a detailed model of the shock strut stroking dynamics in addition to the tire model.

CONCLUSIONS

Tire dynamic parameters play a key part in many design analysis areas for aircraft landing gear systems. Advanced analytical methods to predict tire parameters, such as finite element methods, are needed together with experimental methods for verification of predictions for selected cases and determination of parameters that cannot be determined analytically. Accurate tire data allows more accurate design analyses and correct prediction of dynamic performance of aircraft landing gear. The net result is a more reliable and more efficient system.

REFERENCES

1. Moreland, W. J.: The Story of Shimmy. J. Aeronaut. Sci., Dec. 1974, pp. 793-808.

2. Von Schlippe, V.; and Dietrich, R.: Shimmying of a Pneumatic Wheel. Papers on Shimmy and Rolling Behavior of Landing Gear Presented at Stuttgart Conference, NACA TM-1365, Aug. 1954, pp. 125-160.

3. Edman, J. L.: Experimental Study of Moreland's Theory of Shimmy. WADC Technical Report 56-197, Wright Air Development Center, Wright-Patterson Air Force Base, July 1956.

4. Collins, R. L.; and Black, R. J.: Tire Parameters for Landing Gear Shimmy Studies. AIAA J. Aircraft, May-June 1969, pp. 252-258.

5. Papers on Shimmy and Rolling Behavior of Landing Gear Presented at Stuttgart Conference. NACA TM-1365, Aug. 1954.

6. Smiley, R. F.: Correlation, Evaluation, and Extension of Linearized Theories for Tire Motion and Wheel Shimmy. NACA TN-3632, June 1956.

7. Black, R. J.: Realistic Evaluation of Landing Gear Shimmy Stabilization by Test and Analysis. SAE Paper No. 76-0496, 1976.